

Theoretical studies on the interaction of partial agonists with the 5-HT_{2A} receptor

Maria Elena Silva · Ralf Heim · Andrea Strasser ·
Sigurd Elz · Stefan Dove

Received: 16 August 2010 / Accepted: 28 October 2010 / Published online: 19 November 2010
© Springer Science+Business Media B.V. 2010

Abstract A series of 51 5-HT_{2A} partial agonistic aryl-ethylamines (primary or benzylamines) from different structural classes (indoles, methoxybenzenes, quinazolin-ediones) was investigated by fragment regression analysis (FRA), docking and 3D-QSAR approaches. The data, pEC₅₀ values and intrinsic activities (E_{max}) on rat arteries, show high variability of pEC₅₀ from 4 to 10 and of E_{max} from 15 to 70%. FRA indicates which substructures affect potency or intrinsic activity. The high contribution of halogens in *para* position of phenethylamines to pEC₅₀ points to a specific hydrophobic pocket. Other results suggest the significance of hydrogen bonds of the aryl moiety for activation and the contrary effect of benzyl groups on affinity (increasing) and intrinsic activity (decreasing). Results from fragment regression and data on all available mutants were considered to derive a common binding site at the rat 5-HT_{2A} receptor. After generation and MD simulations of a receptor model based on the β_2 -adrenoceptor structure, typical derivatives were docked, leading to the suggestion of common interactions, e.g., with serines in TM3 and TM5 and with a cluster of aromatic amino acids in TM5 and TM6. The whole series was aligned by docking and minimization of the complexes. The pEC₅₀ values correlate well with Sybyl docking energies and hydrophobicity of the aryl moieties. With this alignment, CoMFA and CoMSIA approaches based on a

training set of 36 and a test set of 15 compounds were performed. The correlation of pEC₅₀ with steric, electrostatic, hydrophobic and H-bond acceptor fields resulted in sufficient fit (q^2 : 0.75–0.8, r^2 : 0.92–0.95) and predictive power (r^2_{pred} : 0.85–0.88). The important interaction regions largely reflect the patterns provided by the putative binding site. In particular, the fit of the aryl moieties and benzyl substituents to two hydrophobic pockets is evident.

Keywords 5-HT_{2A} receptor · Partial agonists · GPCR modeling · Docking · 3D-QSAR

Abbreviations

h5-HT _{2A} R	Human 5-HT _{2A} receptor
r5-HT _{2A} R	Rat 5-HT _{2A} receptor
h β_2 AR	Human β_2 adrenoceptor
GPCR	G-protein coupled receptor
TM	Transmembranous segment
FRA	Fragment regression analysis
CoMFA	Comparative molecular field analysis
CoMSIA	Comparative molecular similarity index analysis
PLS	Partial least squares analysis
PC	Principal component
3D-QSAR	Three-dimensional quantitative structure–activity relationships

M. E. Silva · R. Heim · A. Strasser · S. Elz · S. Dove (✉)
Institute of Pharmacy, University of Regensburg,
93040 Regensburg, Germany
e-mail: Stefan.Dove@chemie.uni-regensburg.de

Present Address:

M. E. Silva
Institute of Pharmacology and Toxicology, Paracelsus Medical
University Salzburg, Strubergasse 21, 5020 Salzburg, Austria

Introduction

5-HT_{2A} receptors (5-HT_{2A}R) [1] belong to the G-protein coupled receptor super-family (GPCR) and mediate the effects of the endogenous neurotransmitter serotonin

(5-hydroxytryptamine, 5-HT) [2, 3]. GPCRs are characterized by a conserved transmembrane domain consisting of seven α -helices (TM1–7). The extracellular face consists of an N-terminal fragment (NT) and three loops (E1–3) linking TMs 2 and 3, 4 and 5, as well as 6 and 7, respectively. Three intracellular loops (I1–3) connect TMs 1 and 2, 3 and 4, as well as 5 and 6. The C-terminal segment (CT) begins with a short loop and an additional conserved α -helix (H8). 5-HT_{2A}Rs are coupled to the G_{αq}/G_{α11} signal transduction pathway with activation of phospholipase C.

5-HT_{2A}R mediated signal transduction affects a large number of key physiological processes including vascular and nonvascular smooth muscle contraction, platelet aggregation, perception and affective behaviour [4, 5] (for review, see [6]). Additionally, 5-HT_{2A} receptors represent a major site of action of hallucinogens like ergolines (e.g., lysergic acid diethylamine), phenylisopropylamines (e.g., 1-(4-iodo-2,5-dimethoxyphenyl)-isopropylamine, DOI) and substituted tryptamines (e.g., *N,N*-dimethyltryptamine, DMT). In most assays, these compounds act as partial 5-HT_{2A}R agonists. The affinity of the endogenous agonist 5-HT is relatively low ($pK_i \sim 6$). Dimethoxyphenylalkylamines like mescaline and 1-(4-bromo-2,5-dimethoxyphenyl)-isopropylamine (DOB) are more affine and potent 5HT_{2A}R agonists. Introduction of larger, especially benzyl substituents at the amine nitrogen leads to partial agonists that are up to 400–1,400 times more active than 5-HT due to higher affinity [7, 8]. This “affinity-conferring” principle may be applied to other structural classes as indoles and quinazolinones.

To obtain still more potent 5-HT_{2A}R agonists and to investigate structure–activity relationships (SAR), a series of more than 60 compounds was synthesized in our lab and tested for 5-HT_{2A}R agonistic potency (pEC_{50}) and intrinsic activity (E_{max}) on rat arteries [8–14]. The series comprises diverse primary and secondary aryethylamines belonging to different structural classes according to the aryl moiety (indole, benzene and quinazolinone derivatives), and shows high variability of pEC_{50} from 4 to 10 and of E_{max} from 15 to 71%.

The aim of the present study was to analyze the quantitative structure–activity relationships (QSAR) of these compounds and to predict 5-HT_{2A}R binding modes. Following a hierarchic strategy, different methods have been applied: fragment regression analysis (FRA), receptor modeling, docking studies and 3D-QSAR approaches [comparative molecular field analysis (CoMFA) and comparative molecular similarity index analysis (CoMSIA)].

Generally, all these methods contribute to the investigation of ligand–receptor interactions. FRA provides information about which substructures and substituents strongly affect affinity and potency and, by this, which kinds of effect may play a role in a certain position. On the

other hand, homology models of the rat (r5-HT_{2A}R) and the human (h5-HT_{2A}R) 5-HT_{2A} receptor based on the crystal structure of the human β_2 adrenoceptor (h β_2 AR) [15, 16] together with results from in vitro mutagenesis studies predict the location, topology and the amino acids of the agonist binding site. The docking of representative compounds of each structural class into this site generates common and/or individual ligand–receptor interactions, which must not disagree with the QSAR from the FRA and with the ligand-binding properties of the receptor mutants, and provides the templates for a common, structure-based alignment of the whole series. Finally, CoMFA and CoMSIA approaches are to analyze the QSAR in detail, leading to interaction fields which may be projected onto the binding site model and, by this, refine the exploration of the SAR and the ligand–receptor interactions.

Methods

Data set

The 5-HT_{2A} partial agonists considered in this study and their biological data were obtained from Elz et al. [8–14]. r5-HT_{2A}R agonistic potency (pEC_{50}) and intrinsic activity (E_{max}) were measured by a functional in vitro assay using cylindric segments from rat tail arteries. It is assumed that pEC_{50} values largely reflect r5-HT_{2A}R affinity.

The structures and the data of the 51 partial agonists analyzed by QSAR approaches are given in Table 1. The compounds belong to three different structural classes—(I) 2-(1*H*-indol-3-yl)-, (P) 2-phenyl- and (Q) 2-(quinazoline-2,4(1*H*,3*H*)-dione-3-yl)ethylamines.

5-HT_{2A}R models

Three-dimensional models of the r5-HT_{2A}R and the h5-HT_{2A}R were generated by homology modeling. The present pharmacological data were from the rat; the h5-HT_{2A}R model was only used for investigations about the possible role of Ser242 (r5-HT_{2A}R: Ala242) for agonist binding. Sequences were retrieved from the Swissprot database (P28223 and P14842, respectively) [17]. The homology between both receptor species is very high. The most diverse portions are at the N- and C-terminus. The identity of the sequences considered in the models amounts to 98.5%, only five amino acids in TM1, TM3, TM5, I3 and E3 are different (Fig. 1).

For the construction of the r5-HT_{2A}R model, the crystal structure of the h β_2 AR (h β_2 AR-T4L, PDB 2rh1) [15] was used as template after excision of the lysozyme adduct. The sequence of the h β_2 AR was mutated into that of the r5-HT_{2A}R at positions without gaps and deletions, i.e. TM1

Table 1 Structure, agonistic potency (pEC₅₀) and efficacy (E_{max}) of r5-HT_{2A}R partial agonistic arylethylamines

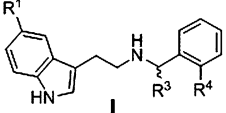
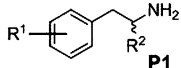
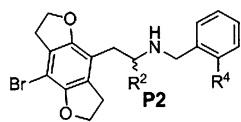
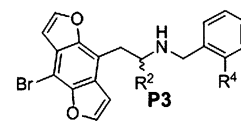
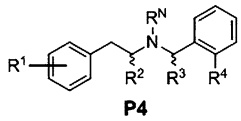
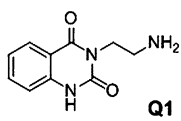
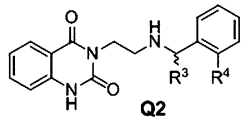
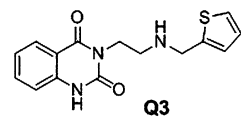
<div><div></div><div></div><div></div><div></div><div></div><div></div><div></div><div></div></div>														Nr. ^a	Class	R ¹	R ²	R ³ (R ^N) ^b	R ⁴	pEC ₅₀	E _{max} [%] ^c	log E _{max}	log P ^d	Residuals			FRA ^e	CoMFA ^f	CoMSIA ^f	5HT	–	–	–	–	–	7.00 ± 0.03	100 ± 10							1*	I	H	–	H	H	6.39 ± 0.07	26 ± 3	1.415	2.62	0.44	0.35	0.26	2		H	–	H	OH	6.87 ± 0.08	47 ± 3	1.672	2.62	0.03	–0.14	–0.37	3		H	–	H	OMe	6.81 ± 0.06	44 ± 2	1.643	2.62	0.12	0.44	0.33	4		H	–	H	OEt	6.06 ± 0.08	19 ± 1	1.279	2.62	–0.20	0.20	–0.20	5		H	–	Me	OMe	6.20 ± 0.10	27 ± 4	1.431	2.62	–0.11	–0.23	–0.26	6		OMe	–	H	H	7.00 ± 0.07	30 ± 3	1.477	2.40	0.26	0.38	0.58	7		OMe	–	H	OH	7.50 ± 0.07	38 ± 2	1.580	2.40	–0.13	0.08	–0.05	8*		OMe	–	H	OMe	7.08 ± 0.03	54 ± 2	1.732	2.40	–0.40	0.03	0.28	9	P1	2,5-(OMe) ₂	H	–	–	4.41 ± 0.22	47 ± 2	1.672	2.64	–0.80	–0.35	–1.14	10		2,5-(OMe) ₂ , 4-Br	H	–	–	7.20 ± 0.03	58 ± 3	1.763	3.50	–0.45	0.17	0.11	11*		2,5-(OMe) ₂ , 4-Br	Me	–	–	7.99 ± 0.06	71 ± 3	1.851	3.50	0.94	0.60	0.97	12		2,5-(OMe) ₂ , 4-I	Me	–	–	8.13 ± 0.05	68 ± 1	1.833	4.07	0.59	0.33	0.35	13		2,3,4-(OMe) ₃	H	–	–	5.88 ± 0.07	59 ± 5	1.771	1.74	0.05	–0.23	0.02	14		2,4,5-(OMe) ₃	H	–	–	5.86 ± 0.04	60 ± 4	1.778	2.12	–0.12	–0.22	0.45	15	P2	Br	H	–	OH	9.87 ± 0.09	34 ± 2	1.531	3.28	0.07	–0.05	–0.19	16		Br	H	–	OMe	10.15 ± 0.07	27 ± 3	1.431	3.28	0.50	0.77	0.78	17		Br	Me	–	OMe	8.33 ± 0.05	17 ± 3	1.230	3.28	–0.71	–0.86	–0.77	18*	P3	Br	H	–	OH	9.94 ± 0.08	24 ± 4	1.380	3.40	0.14	0.92	0.66	19	P4 ^b	2,5-(OMe) ₂	H	H	OMe	7.73 ± 0.03	40 ± 2	1.602	2.64	0.64	0.49	0.39	20*		2,5-(OMe) ₂ , 4-Br	H	H	OH	9.66 ± 0.09	35 ± 3	1.544	3.50	–0.02	0.12	0.14	21		2,5-(OMe) ₂ , 4-Br	H	H	OMe	9.58 ± 0.05	38 ± 2	1.580	3.50	0.05	0.37	0.70	22		2,5-(OMe) ₂ , 4-Br	H	(R)-Me	OMe	8.24 ± 0.16	29 ± 3	1.462	3.50	0.12	–0.32	–0.22	23		2,5-(OMe) ₂ , 4-Br	H	(S)-Me	OMe	9.32 ± 0.04	26 ± 2	1.415	3.50	0.17	0.32	0.58	24		2,5-(OMe) ₂ , 4-Br	H	(N-Me) ^b	OMe	7.41 ± 0.09	27 ± 3	1.431	3.50	0	–0.03	–0.44	25*		2,5-(OMe) ₂ , 4-Br	Me	H	OMe	8.10 ± 0.06	20 ± 3	1.301	3.50	–0.82	–1.19	–0.59	26		2,5-(OMe) ₂ , 4-I	H	H	OH	10.13 ± 0.07	29 ± 4	1.462	4.07	–0.04	0.21	–0.16	27		2,5-(OMe) ₂ , 4-I	H	H	OMe	10.09 ± 0.08	30 ± 5	1.477	4.07	0.07	0.51	0.43	28		2,5-(OMe) ₂ , 4-I	H	(R)-Me	OMe	8.41 ± 0.07	28 ± 4	1.447	4.07	–0.20	–0.50	–0.84	29*		2,5-(OMe) ₂ , 4-I	H	(S)-Me	OMe	9.21 ± 0.06	29 ± 4	1.462	4.07	–0.43	–0.20	–0.31	30*		2,5-(OMe) ₂ , 4-CF ₃	H	H	OH	9.13 ± 0.08	28 ± 4	1.447	3.46	–0.02	–0.69	–0.41	31		2,5-(OMe) ₂ , 4-CF ₃	H	H	OMe	9.02 ± 0.09	36 ± 3	1.556	3.46	0.02	–0.25	0.13	32		3,4-(OMe) ₂	H	H	OMe	6.47 ± 0.05	44 ± 2	1.643	2.18	–0.27	–0.42	–0.25	33*		3,5-(OMe) ₂	H	H	OMe	7.02 ± 0.03	40 ± 1	1.602	2.90	0.27	–0.49	0.21	34		2,6-(OMe) ₂	H	H	OMe	7.81 ± 0.05	31 ± 4	1.491	2.75	–0.10	–0.28	–0.53	35		2,3,4-(OMe) ₃	H	H	OMe	7.66 ± 0.04	50 ± 2	1.699	1.74	–0.05	–0.22	–0.21	36*		2,4,5-(OMe) ₃	H	H	OMe	8.14 ± 0.04	57 ± 5	1.756	2.12	0.28	–0.03	0.87	37		2,4,6-(OMe) ₃	H	H	OMe	8.78 ± 0.05	49 ± 2	1.690	2.79	0.10	–0.50	0.55	38		2-Br	H	H	OMe	6.62 ± 0.02	26 ± 2	1.415	3.50	0	0.41	0.21
Nr. ^a	Class	R ¹	R ²	R ³ (R ^N) ^b	R ⁴	pEC ₅₀	E _{max} [%] ^c	log E _{max}	log P ^d	Residuals																																																																																																																																																																																																																																																																																																																																																																																																																																																																																																																																															
										FRA ^e	CoMFA ^f	CoMSIA ^f																																																																																																																																																																																																																																																																																																																																																																																																																																																																																																																																													
5HT	–	–	–	–	–	7.00 ± 0.03	100 ± 10																																																																																																																																																																																																																																																																																																																																																																																																																																																																																																																																																		
1*	I	H	–	H	H	6.39 ± 0.07	26 ± 3	1.415	2.62	0.44	0.35	0.26																																																																																																																																																																																																																																																																																																																																																																																																																																																																																																																																													
2		H	–	H	OH	6.87 ± 0.08	47 ± 3	1.672	2.62	0.03	–0.14	–0.37																																																																																																																																																																																																																																																																																																																																																																																																																																																																																																																																													
3		H	–	H	OMe	6.81 ± 0.06	44 ± 2	1.643	2.62	0.12	0.44	0.33																																																																																																																																																																																																																																																																																																																																																																																																																																																																																																																																													
4		H	–	H	OEt	6.06 ± 0.08	19 ± 1	1.279	2.62	–0.20	0.20	–0.20																																																																																																																																																																																																																																																																																																																																																																																																																																																																																																																																													
5		H	–	Me	OMe	6.20 ± 0.10	27 ± 4	1.431	2.62	–0.11	–0.23	–0.26																																																																																																																																																																																																																																																																																																																																																																																																																																																																																																																																													
6		OMe	–	H	H	7.00 ± 0.07	30 ± 3	1.477	2.40	0.26	0.38	0.58																																																																																																																																																																																																																																																																																																																																																																																																																																																																																																																																													
7		OMe	–	H	OH	7.50 ± 0.07	38 ± 2	1.580	2.40	–0.13	0.08	–0.05																																																																																																																																																																																																																																																																																																																																																																																																																																																																																																																																													
8*		OMe	–	H	OMe	7.08 ± 0.03	54 ± 2	1.732	2.40	–0.40	0.03	0.28																																																																																																																																																																																																																																																																																																																																																																																																																																																																																																																																													
9	P1	2,5-(OMe) ₂	H	–	–	4.41 ± 0.22	47 ± 2	1.672	2.64	–0.80	–0.35	–1.14																																																																																																																																																																																																																																																																																																																																																																																																																																																																																																																																													
10		2,5-(OMe) ₂ , 4-Br	H	–	–	7.20 ± 0.03	58 ± 3	1.763	3.50	–0.45	0.17	0.11																																																																																																																																																																																																																																																																																																																																																																																																																																																																																																																																													
11*		2,5-(OMe) ₂ , 4-Br	Me	–	–	7.99 ± 0.06	71 ± 3	1.851	3.50	0.94	0.60	0.97																																																																																																																																																																																																																																																																																																																																																																																																																																																																																																																																													
12		2,5-(OMe) ₂ , 4-I	Me	–	–	8.13 ± 0.05	68 ± 1	1.833	4.07	0.59	0.33	0.35																																																																																																																																																																																																																																																																																																																																																																																																																																																																																																																																													
13		2,3,4-(OMe) ₃	H	–	–	5.88 ± 0.07	59 ± 5	1.771	1.74	0.05	–0.23	0.02																																																																																																																																																																																																																																																																																																																																																																																																																																																																																																																																													
14		2,4,5-(OMe) ₃	H	–	–	5.86 ± 0.04	60 ± 4	1.778	2.12	–0.12	–0.22	0.45																																																																																																																																																																																																																																																																																																																																																																																																																																																																																																																																													
15	P2	Br	H	–	OH	9.87 ± 0.09	34 ± 2	1.531	3.28	0.07	–0.05	–0.19																																																																																																																																																																																																																																																																																																																																																																																																																																																																																																																																													
16		Br	H	–	OMe	10.15 ± 0.07	27 ± 3	1.431	3.28	0.50	0.77	0.78																																																																																																																																																																																																																																																																																																																																																																																																																																																																																																																																													
17		Br	Me	–	OMe	8.33 ± 0.05	17 ± 3	1.230	3.28	–0.71	–0.86	–0.77																																																																																																																																																																																																																																																																																																																																																																																																																																																																																																																																													
18*	P3	Br	H	–	OH	9.94 ± 0.08	24 ± 4	1.380	3.40	0.14	0.92	0.66																																																																																																																																																																																																																																																																																																																																																																																																																																																																																																																																													
19	P4 ^b	2,5-(OMe) ₂	H	H	OMe	7.73 ± 0.03	40 ± 2	1.602	2.64	0.64	0.49	0.39																																																																																																																																																																																																																																																																																																																																																																																																																																																																																																																																													
20*		2,5-(OMe) ₂ , 4-Br	H	H	OH	9.66 ± 0.09	35 ± 3	1.544	3.50	–0.02	0.12	0.14																																																																																																																																																																																																																																																																																																																																																																																																																																																																																																																																													
21		2,5-(OMe) ₂ , 4-Br	H	H	OMe	9.58 ± 0.05	38 ± 2	1.580	3.50	0.05	0.37	0.70																																																																																																																																																																																																																																																																																																																																																																																																																																																																																																																																													
22		2,5-(OMe) ₂ , 4-Br	H	(R)-Me	OMe	8.24 ± 0.16	29 ± 3	1.462	3.50	0.12	–0.32	–0.22																																																																																																																																																																																																																																																																																																																																																																																																																																																																																																																																													
23		2,5-(OMe) ₂ , 4-Br	H	(S)-Me	OMe	9.32 ± 0.04	26 ± 2	1.415	3.50	0.17	0.32	0.58																																																																																																																																																																																																																																																																																																																																																																																																																																																																																																																																													
24		2,5-(OMe) ₂ , 4-Br	H	(N-Me) ^b	OMe	7.41 ± 0.09	27 ± 3	1.431	3.50	0	–0.03	–0.44																																																																																																																																																																																																																																																																																																																																																																																																																																																																																																																																													
25*		2,5-(OMe) ₂ , 4-Br	Me	H	OMe	8.10 ± 0.06	20 ± 3	1.301	3.50	–0.82	–1.19	–0.59																																																																																																																																																																																																																																																																																																																																																																																																																																																																																																																																													
26		2,5-(OMe) ₂ , 4-I	H	H	OH	10.13 ± 0.07	29 ± 4	1.462	4.07	–0.04	0.21	–0.16																																																																																																																																																																																																																																																																																																																																																																																																																																																																																																																																													
27		2,5-(OMe) ₂ , 4-I	H	H	OMe	10.09 ± 0.08	30 ± 5	1.477	4.07	0.07	0.51	0.43																																																																																																																																																																																																																																																																																																																																																																																																																																																																																																																																													
28		2,5-(OMe) ₂ , 4-I	H	(R)-Me	OMe	8.41 ± 0.07	28 ± 4	1.447	4.07	–0.20	–0.50	–0.84																																																																																																																																																																																																																																																																																																																																																																																																																																																																																																																																													
29*		2,5-(OMe) ₂ , 4-I	H	(S)-Me	OMe	9.21 ± 0.06	29 ± 4	1.462	4.07	–0.43	–0.20	–0.31																																																																																																																																																																																																																																																																																																																																																																																																																																																																																																																																													
30*		2,5-(OMe) ₂ , 4-CF ₃	H	H	OH	9.13 ± 0.08	28 ± 4	1.447	3.46	–0.02	–0.69	–0.41																																																																																																																																																																																																																																																																																																																																																																																																																																																																																																																																													
31		2,5-(OMe) ₂ , 4-CF ₃	H	H	OMe	9.02 ± 0.09	36 ± 3	1.556	3.46	0.02	–0.25	0.13																																																																																																																																																																																																																																																																																																																																																																																																																																																																																																																																													
32		3,4-(OMe) ₂	H	H	OMe	6.47 ± 0.05	44 ± 2	1.643	2.18	–0.27	–0.42	–0.25																																																																																																																																																																																																																																																																																																																																																																																																																																																																																																																																													
33*		3,5-(OMe) ₂	H	H	OMe	7.02 ± 0.03	40 ± 1	1.602	2.90	0.27	–0.49	0.21																																																																																																																																																																																																																																																																																																																																																																																																																																																																																																																																													
34		2,6-(OMe) ₂	H	H	OMe	7.81 ± 0.05	31 ± 4	1.491	2.75	–0.10	–0.28	–0.53																																																																																																																																																																																																																																																																																																																																																																																																																																																																																																																																													
35		2,3,4-(OMe) ₃	H	H	OMe	7.66 ± 0.04	50 ± 2	1.699	1.74	–0.05	–0.22	–0.21																																																																																																																																																																																																																																																																																																																																																																																																																																																																																																																																													
36*		2,4,5-(OMe) ₃	H	H	OMe	8.14 ± 0.04	57 ± 5	1.756	2.12	0.28	–0.03	0.87																																																																																																																																																																																																																																																																																																																																																																																																																																																																																																																																													
37		2,4,6-(OMe) ₃	H	H	OMe	8.78 ± 0.05	49 ± 2	1.690	2.79	0.10	–0.50	0.55																																																																																																																																																																																																																																																																																																																																																																																																																																																																																																																																													
38		2-Br	H	H	OMe	6.62 ± 0.02	26 ± 2	1.415	3.50	0	0.41	0.21																																																																																																																																																																																																																																																																																																																																																																																																																																																																																																																																													

Table 1 continued

Nr. ^a	Class	<i>R</i> ¹	<i>R</i> ²	<i>R</i> ³ (<i>R</i> ^N) ^b	<i>R</i> ⁴	pEC ₅₀ ^c	<i>E</i> _{max} [%] ^c	log <i>E</i> _{max}	log <i>P</i> ^d	Residuals		
										FRA ^e	CoMFA ^f	CoMSIA ^f
39*		3-Br	H	H	OMe	6.90 ± 0.04	38 ± 4	1.580	3.49	0	<i>0.56</i>	<i>0.35</i>
40	Q1	–	–	–	–	4.18 ± 0.09	46 ± 4	1.663	1.33	–0.21	0.22	–0.14
41*	Q2	–	–	H	H	4.84 ± 0.06	33 ± 3	1.519	1.33	–0.70	<i>–0.84</i>	<i>–0.87</i>
42*		–	–	H	Me	5.52 ± 0.13	22 ± 3	1.342	1.33	0	<i>–0.72</i>	<i>–0.55</i>
43*		–	–	H	Cl	5.08 ± 0.05	15 ± 2	1.176	1.33	0	<i>0.03</i>	<i>0.30</i>
44		–	–	H	Br	5.05 ± 0.03	16 ± 1	1.204	1.33	0	0.09	0.55
45		–	–	H	NH ₂	5.05 ± 0.05	54 ± 2	1.732	1.33	0	–0.47	–0.66
46		–	–	H	OH	6.38 ± 0.09	51 ± 3	1.708	1.33	–0.04	–0.33	–0.55
47		–	–	H	OMe	6.58 ± 0.06	49 ± 4	1.690	1.33	0.31	0.41	0.40
48*		–	–	(<i>R</i>)-Me	OMe	4.93 ± 0.08	11 ± 1	1.041	1.33	0.07	<i>–1.11</i>	<i>–1.00</i>
49		–	–	(<i>S</i>)-Me	OMe	6.26 ± 0.07	41 ± 3	1.613	1.33	0.37	0.03	0.23
50		–	–	H	OEt	6.05 ± 0.05	34 ± 1	1.531	1.33	0.20	0.17	–0.05
51	Q3	–	–	–	–	5.47 ± 0.03	22 ± 2	1.342	1.33	0	–0.20	0.22

^a Compounds with asterisk (*)—members of the test set in 3D-QSAR analyses

^b *R*^N denotes an N-methyl group in a tertiary amine (compound **24**)

^c r5-HT_{2A}R agonistic potency (pEC₅₀) and intrinsic activity (*E*_{max}) measured by a functional in vitro assay using cylindric segments from rat tail arteries

^d log *P* values of arylmethyl fragments (replacement of the ethylamine moiety by a methyl group), calculated with ACDLabs 12.0

^e Residuals pEC₅₀–pEC₅₀(calc) from fragment regression analysis; zeros (0) denote compounds with unique fragments

^f Residuals pEC₅₀–pEC₅₀(calc or pred) from final CoMFA and CoMSIA models, respectively; prediction errors of test set compounds are in italics

to TM7, intracellular loops I1 and I2, and the C-terminus (C-Ter) up to Cys397, using the alignment shown in Fig. 1. Since the 5-HT_{2A}R N- and C-termini are longer than in the hβ₂AR, and since the homology of the terminal sequences is low, the prediction of the chains preceding TM1 and following H8 would be highly speculative. Therefore, the first 69 N-terminal and the last 74 C-terminal residues were not considered in the construction of the model. The remaining intracellular and extracellular loops (E1, E2, E3 and I3) were filled by the Biopolymer loop search facility in Sybyl 7.3 (Tripos, St. Louis, MO) with appropriate segments from a binary protein database based on PDB structures. Side chains and hydrogens were added using the Biopolymer module of Sybyl 7.3.

The resulting model was prepared for optimization by adding hydrogens and providing atoms with Amber-FF99 charges [18]. Bad contacts of side chains were removed using the Lovell rotamer library [19]. Subsequently, the model was roughly minimized (25 cycles steepest descent with fixed TM backbone, 100 cycles Powell conjugated gradient, Amber-FF99 force field [18], distant dependent dielectric constant $\epsilon = 4$) and checked for inconsistencies of the local geometry with Sybyl ProTable. Molecular dynamics (MD) simulations were performed following a protocol published in detail elsewhere [20]. In brief, the model was embedded into an environment consisting of 93 1-palmitoyl-2-oleoyl-phosphatidylcholine molecules,

14,429 intracellular and extracellular water molecules, and 8 Na⁺ and 24 Cl[–] ions to achieve electroneutrality, and the whole complex was minimized. The 1.35 ns equilibrium phase of the MD was divided into one 250 ps and eleven 100 ps cycles with gradually descending constraints for the backbone and the side chain atoms. Then, a 1 ns productive phase without constraints was performed. The simulations were carried out at 310 K and 1 atmosphere with Berendsen, temperature, and pressure coupling using the software package GROMACS 3.2 [21] with the ffG53A6 force field [22].

The final snapshot of the MD simulation was minimized (SYBYL 7.3, Amber-FF99 force field, $\epsilon = 4$, end RMS gradient 0.05 kcal mol^{–1}). An h5-HT_{2A}R model was generated from the final MD structure by mutation of the five amino acids differing between the rat and human model sequences, followed by the same minimization protocol.

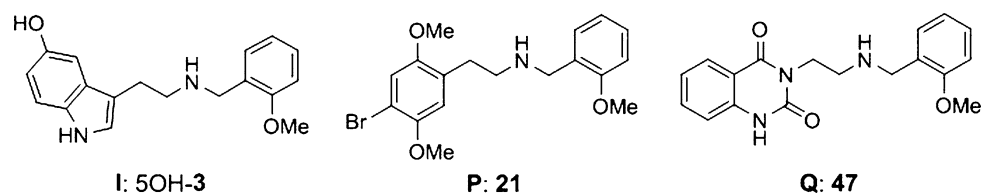
Ligand structure generation and docking

To explore the putative binding sites and common ligand-receptor interactions, docking approaches with one representative compound from each structural class (**I**, **P**, **Q**) were performed first. The selection was based on high potency, recognition of probably essential interactions and on the FRA results. Among the substituents at the amino

Fig. 1 Sequence alignment of the h5-HT_{2A}R and the r5-HT_{2A}R with the hβ₂AR; *dots* in the hβ₂AR sequence: identity with the r5-HT_{2A}R; *grey shading*: most conserved position (nr. 50 according to the Ballesteros numbering scheme [31]) in each TM; *lines* above the sequences: spans of the TMs; *bold letters*: positions where the r5-HT_{2A}R differs from the h5-HT_{2A}R; *bold and italic letters*: N- and C-termini of the models

			NT
h5HT2A	1	MDILCEENTSLSSTTNSLMQLNDDTRLYSNDFNSGEANTSDAFNWTVDSENRTNLSCEGLSPSC	
r5HT2A	1	MEILCEDNISLSSSIPNSLMQLG GDG PRLYHNDFN SRD ANTSEASNWT IDA ENRTNLSCEGL PP TC	
hβ2AR	1	-----MGQPGNGS.F---LL.P..SHAPDHDVTQQR-	
		TM1 I1 TM2	
h5HT2A	66	LSLL HL QEKNSALLTAVVILTIAGN IL VIMAVSLEK KL Q NAT NYFLMSLA IA DM LL GFLVMPV	
r5HT2A	66	LS IL HL QEKNSALLT TV VILTIAGN IL VIMAVSLEK KL Q NAT NYFLMSLA IA DM LL GFLVMPV	
hβ2AR	29	---- DEV VVVG MG IVMSLIVLAIVF..V...T.IAKFER..TV...IT...C..LVM.LA.V.F	
		E1 TM3 I2	
h5HT2A	131	SMLTILYGYRWPLPSKLC AV WILYDLVLFSTASIMHLCAISLD RY VAIQNP I HSR FN SRTKAFLK	
r5HT2A	131	SMLTILYGYRWPLPSKLC AV WILYDLVLFSTASIMHLCAISLD RY VAIQNP I HSR FN SRTKAFLK	
hβ2AR	90	GAAH..MK-M.TFG N W.EF.TSI...CV...ET..V.AV..F..TS.FKYQ S LLTKN..RVI	
		TM4 E2 TM5	
h5HT2A	196	IIAV WT ISVGISMP IP VFGLQDD S ---KVF---KEGSCLLA-DDNFVLIGSFV S FFI PL TMIVIT	
r5HT2A	196	IIAV WT ISVGISMP IP VFGLQDD S ---KVF---KEGSCLLA-DDNFVLIGSFV A FFI PL TMIVIT	
hβ2AR	154	.LM..IV.GLT.FLPIQ M HWYRATHQ E A I NCYAN.TC.DFFT N QAY A IAS.I.S.YV..V...FV	
		I3	
h5HT2A	254	YFLT IK SLQKEATLCVSDLGTRAKLASFSFLPQSSLSSEKLFQ RS I H REP GS YTGRRTMQ S ISNE	
r5HT2A	254	YFLT IK SLQKEATLCVSD L STRAKLASFSFLPQSSLSSEKLFQ RS I H REP GS YTGRRTMQ S ISNE	
hβ2AR	219	.SRV F Q E AKRQLQKIDKSEG-.FHVQNL.QVE.DGRTG-----HGL..SSK F CLK..	
		TM6 E3 TM7	
h5HT2A	319	QKACKVLGIVFFLFVVMWC PF FITNIMAVICKESCNE D VIGALLNVFVWIGYLSSAVNPLVYTLF	
r5HT2A	319	QKACKVLGIVFFLFVVMWC PF FITNIMAVICKESCNE V VIGALLNVFVWIGYLSSAVNPLVYTLF	
hβ2AR	269	H..L.T...IMGT.TLC.L...V..VH..QD---LIR-KEYV I LLN...VN.GF...I.CRS	
		H8 CT	
h5HT2A	384	NKTYRS A FSRYIQ C QYKEN K PLQLILVNTIPALAYKSSQLQMGQK N SKQDAKT TD ND C SMVAL	
r5HT2A	384	NKTYRS A FSRYIQ C QYKEN R KPLQLILVNTIPALAYKSSQLQ V GQK N S Q ED A EQ IV DD C SMV T L	
hβ2AR	330	P-DF.I..Q EL LC L RRSS L KAYGNGYSS.GN---TGEQ.GYH.E.E.ENK L LC.DLPGTE D F.GH	
h5HT2A	449	GKQHSE E ASKD NS DGVNEK V SCV	
r5HT2A	449	GK Q QSE N CT DN I ET VNEK V SCV	
hβ2AR	391	QGTVP S D.ID S QGRNC ST ND.LL	

Fig. 2 Representative compounds used for docking studies and as templates for the alignment



moiety which were similarly varied in each subseries (see Table 1), a 2-methoxybenzyl group is optimal. Therefore, each class was represented by a compound containing this substituent. The selected structures, 5OH-3 (**I**), additionally representing interaction of a 5-OH substituent like in 5-HT), **21** (**P**) and **47** (**Q**), are shown in Fig. 2.

The molecules were constructed using Sybyl 7.3. All structures were assumed to be protonated under physiological conditions. AmberFF99 atom types and Gasteiger-Hueckel charges were assigned to the ligands. The docking modes (bioactive conformations) were derived from the suggested common binding site in order to get a structure-based alignment. Information about the location of essential amino acids resulted from site-directed mutagenesis studies. The highly conserved Asp155^{3,32} [23, 24], the serines Ser159^{3,36}, Ser239^{5,43}, Ser242^{5,46} (h5-HT_{2A}R,

Ala242 in r5-HT_{2A}R) [25–27] and the phenylalanines Phe243^{5,47}, Phe244^{5,48} [28], Phe340^{6,52} [7, 29, 30] are important for binding and efficacy of agonists and partial agonists at the 5HT_{2A}R. Phe339^{6,51} is suggested to interact with the N-benzyl substituents [7] (Superscripts indicate the generic numbering scheme of amino acids in TMs 1–7 proposed by Ballesteros and Weinstein [31]).

The three ligands were manually docked into the binding site considering the mutagenesis data and the QSAR obtained from fragment regression analysis. During docking, the conformations of the ligands were varied in order to get maximal overlap of the scaffolds and shared interactions with the essential amino acids described above. The complexes were optimized by a stepwise approach: (1) 100 cycles AmberFF99 force field with fixed ligands (distant dependent dielectric constant 4, steepest descent method),

followed by minimization with the Powell algorithm (final RMS gradient of $0.05 \text{ kcal mol}^{-1}$), (2) subset minimization of the ligand and a receptor region 6 \AA around using the Tripos force field [32] (distant dependent dielectric constant 1, Powell method, end RMS gradient of $0.05 \text{ kcal mol}^{-1} \text{ \AA}^{-1}$), (3) AmberFF99 force field with fixed ligands (distant dependent dielectric constant 4, Powell method, final RMS gradient $0.01 \text{ kcal mol}^{-1} \text{ \AA}^{-1}$). Range constraints were occasionally applied between Asp155^{3,32} and the protonated nitrogen of the ligands, additionally for cpd. **21** between Ser159^{3,36} and the 2-OCH₃ group, and for cpds. 5OH-3 and **21** between Ser239^{5,43} and the 5-OH and 5-OCH₃ group, respectively.

The other 48 ligands of the series were generated by direct structural modification of the three representative structures, extracted from the complexes with the r5-HT_{2A}R. Using Sybyl 7.3, these templates were changed, provided with Gasteiger-Hueckel charges and merged into the corresponding r5-HT_{2A}R model which resulted from minimization step 1 of the receptor-template complex. According to the moderate stereoselectivity of α -Me-5-HT with eudismic (*S*)/(*R*) ratios of 2 [33] to 23 [34], the (*S*)-isomers were selected in the case of $R^2 = \text{Me}$. Each ligand-receptor complex was optimized with the Tripos force field by subset minimization of the ligand and a receptor region 6 \AA around (distant dependent dielectric constant 1, Powell method, end RMS gradient of $0.05 \text{ kcal mol}^{-1} \text{ \AA}^{-1}$).

For the final ligand-receptor complexes, the binding enthalpy of each compound was calculated with the DOCK function contained in Sybyl 7.3 as sum of the steric and electrostatic interaction energy (Lennard-Jones and Coulomb potential, respectively). The lattice boxes considered in calculations exceeded the binding sites by 3 \AA in each Cartesian direction, and the lattice points were separated by 0.175 \AA in *x*, *y* and *z*.

3D-QSAR approaches

To obtain a common structure-based alignment, the 51 r5-HT_{2A}R partial agonists were extracted from the minimized ligand-receptor complexes without further modification. CoMFA [35] and CoMSIA [36] approaches were performed with the QSAR module of Sybyl 7.3. The grid size was set to 2.0 \AA . Steric and electrostatic CoMFA fields were calculated using the default probe atom, C.3⁺, and energy cutoffs at 30 kcal/mol . In particular, the representation of hydrogen bonds by the electrostatic energy is better with these cutoffs and with quadratic smoothing, since the sampling of H-bond energies is then stopped at $\sim 1.7 \text{ \AA}$ [37]. To reduce sensitivity against grid translations, electrostatics was not dropped inside steric maxima [37]. The calculation of CoMSIA fields (steric,

electrostatic, hydrophobic, H-bond donor and H-bond acceptor field) was based on interactions of the molecules with a common probe atom (radius 1 \AA , charge $+1$, hydrophobicity $+1$, H bond donor and acceptor properties $+1$), using an attenuation factor α of 0.3 in the Gaussian functions.

The docking approaches suggested interactions of the aryl moieties with a hydrophobic pocket. To consider these interactions also in CoMFA which does not provide an explicit hydrophobic field, log *P* values of arylmethyl fragments (replacement of each ethylamine moiety by a methyl group) were calculated with ACDLabs 12.0 (Advanced Chemistry Development Inc., Toronto, ON, Canada, see Table 1).

For correlation of pEC₅₀ values with the standard-scaled field variables and log *P*, Partial Least Squares (PLS) models [38] were generated for a training set of 36 compounds, using the QSAR module in Sybyl 7.3. Different cross-validation techniques [39], leave-one-out with the SAMPLS algorithm, leave-twelve-out (neglecting variables with $s < 0.1$), and progressive scrambling [40] were applied to obtain predictive models and to determine the optimal number of components as follows from the lowest standard error of prediction (*s*_{PRESS}) and sufficient variance contribution of the PCs. The “external” predictivity of the models was checked by a test set of the remaining 15 compounds which were randomly selected with the additional condition that they cover the range of activities and structural variations of the training set [41]. The ratio of the training/test set members of 36/15 is close to the average ratio of 48/17 in more than 60 3D-QSAR applications from the literature [42].

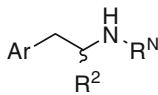
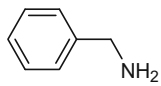
Results and discussion

Fragment regression analysis

“Additivity models” based on indicator variables and calculated by Free-Wilson analysis or FRA are well suited preliminary tools to obtain concise, easily interpretable QSAR results. To a certain degree, these approaches also check the coherence of the biological data and the congenerity of the series and allow the recognition of outliers. For the present FRA of pEC₅₀ and log *E*_{max} values, calculated by the in-house program FRAREG, 2-phenylethylamine was defined as basic structure whose contribution is represented by the intercept of the regression equation. The results are shown in Table 2.

The FRA of pEC₅₀ explains 95.7% of the data variance. The high correlation also depends on the large range of pEC₅₀, the residual standard deviation of 0.49 is of acceptable size compared to the experimental error. The

Table 2 Results of the fragment regression analysis, FRA, of pEC₅₀ and log E_{max}

Pos		Fragment	pEC ₅₀		log E _{max}	
			Increment	95% c.i. ^a	Increment	95% c.i. ^a
Intercept (basic struct.)			3.45	±1.62 ***	1.651	±0.430
Ar						
	Phenyl ^b	0		0		
	Indolyl	1.36	±1.46*	0.101	±0.386	
	Quinazolinedione	0.94	±1.61	0.143	±0.426	
	Benzodifuranyl	1.89	±1.60**	−0.110	±0.425	
	2OMe	0.97	±1.14*	−0.009	±0.301	
	3OMe	0.64	±1.13	0.035	±0.300	
	4OMe	0.77	±0.74**	0.143	±0.196	
	5OMe ^c	0.79	±0.70**	0.074	±0.186	
	6OMe	1.61	±1.16***	0.049	±0.308	
	2Br	1.29	±1.85	−0.064	±0.491	
	3Br	1.57	±1.85*	0.101	±0.491	
	4Br	2.44	±0.81***	0.050	±0.214	
	4I	2.93	±0.85***	0.058	±0.226	
	4CF ₃	1.91	±1.01***	−0.038	±0.268	
R ²	H ^b	0		0		
R ^N	Me	−0.61	±0.67*	−0.085	±0.177	
	H ^b	0		0		
	Benzyl	1.14	±0.83***	−0.320	±0.221***	
	CH ₂ -thiophenyl	1.08	±1.19*	−0.452	±0.314***	
	2OH	0.89	±0.74**	0.139	±0.197	
	2OMe	0.74	±0.73**	0.148	±0.194	
	2OEt	0.31	±0.95	−0.048	±0.252	
	2Me	−0.02	±1.23	−0.132	±0.326	
	2Cl	−0.46	±1.23	−0.298	±0.326*	
	2Br	−0.49	±1.23	−0.270	±0.326*	
	2NH ₂	−0.49	±1.23	0.258	±0.326*	
	(<i>R</i>)-Me	−1.41	±0.72***	−0.289	±0.192***	
	(<i>S</i>)-Me	−0.38	±0.65	−0.119	±0.171	
	N-Me	−2.12	±1.14***	−0.163	±0.303	
	<i>r</i>		0.978	<i>r</i>	0.863	
	<i>r</i> ²		0.957	<i>r</i> ²	0.744	
	<i>s</i>		0.492	<i>s</i>	0.130	
<i>F</i>		20.64***	<i>F</i>	2.69***		

^a 95% confidence intervals and significance levels for *t*-tests of the increments: * > 90%, ** > 95%, *** > 99%^b Fragment belonging to the basic structure (contribution included in the intercept)^c For 5-OMe groups in indolyl and (di-or trisubstituted) phenyl compounds

basic phenylethylamine structure with a contribution of only 3.45 provides a scaffold for activity enhancing substitutions and modifications. The larger aromatic systems (indole, quinazolinedione) increase pEC₅₀ by ca. 1 log unit. The striking and rather additive effect of methoxy

substituents at the indole (5-OMe) and the phenyl moiety is congruent with the high contribution of the benzodifuran moiety. It can be suggested that at least one oxygen atom is involved in a polar interaction with the receptor. The second striking result is the large contribution of lipophilic

substituents like halogens and CF_3 in *para* position of phenylethylamine derivatives (1.9–2.9 pEC_{50} units), indicating fit to a specific hydrophobic pocket.

On average, methyl groups in α -position of the ethyl side chain decrease activity. However, the effect of α -Me depends on the nature of the amino group: if one considers the pEC_{50} values and residuals (see Table 1), it becomes obvious that the methyl branch is favourable in primary amines (cpds. **11** and **12**) and unfavourable in secondary benzylamines (cpds. **17** and **25**). This different behavior may be simply due to a potential interaction of the α -Me group with the receptor which is not possible in the case of a bulky R^N moiety because of restricted degrees of freedom for fit. A methyl group as part of a tertiary amine strongly lowers activity.

It is well known that aralkyl groups as R^N substituents lead to high affinity of agonists and antagonists for many biogenic amine receptors. Corresponding to this quite general rule, secondary benzylamines are more than one pEC_{50} unit more active at the $\text{r5-HT}_{2A}\text{R}$ than their NH_2 analogs. An *ortho*-OH or -OMe substituent at the phenyl ring further increases activity, so that the overall contribution of 2-OMe- or 2-OH-benzyl groups approaches 2 log units. The effect of other *ortho* substituents is not significant. It may be suggested that the oxygen is involved in an H bond with the receptor. Among the stereoisomeric methylbenzyl groups, the *S* isomer is equiactive compared to benzyl, whereas the *R* configuration leads to reduction of the activity by nearly 1.5 pEC_{50} units.

There is no real outlier in the FRA of pEC_{50} even if the rather strong criterion $\text{abs}(\text{residual}) > 2\text{ s}$ is applied. However, eight compounds cannot be validated because of unique substituents (residuals of 0, see Table 1). Three of the four largest residuals are due to the different α -methyl effect (see above). The fourth “outlier” is cpd. **9** (2,5-dimethoxyphenylethylamine), its activity is by 0.8 pEC_{50} units lower than calculated.

The analysis of $\log E_{\text{max}}$ should provide some detailed information about structure-efficacy relationships. However, this approach suffers from the low standard deviation of the dependent variable (range of $\log E_{\text{max}}$ from 1.04 to 1.85, s : 0.18). The FRA model explains $\sim 75\%$ of the variance. Therefore, conclusions from the analysis are restricted to some more pronounced effects. The contribution of 2-phenylethylamine as basic structure corresponds to an intrinsic activity of 45%. Larger aromatic systems (indole, quinazolinodione) and methoxy substituents (except 2-OMe) only slightly increase $\log E_{\text{max}}$. No contribution is significantly different from zero at the 95% level. It seems that all arylethylamine moieties except those with a benzodifuran group are approximately equipotent in their ability to induce the transition from the inactive to the active receptor state. In the present series of partial

agonists, appropriate substitution can improve this potential by only 0.17 $\log E_{\text{max}}$ units.

Strikingly, $\log E_{\text{max}}$ is significantly reduced in the case of the secondary amines. The same groups (benzyl, CH_2 -2-thiophenyl) which strongly increase pEC_{50} reduce the intrinsic activity. This effect may be slightly counterbalanced by *ortho* benzyl substituents (OH, OMe, NH_2), indicating the role of polar interactions at this position also for receptor activation. On the other hand, *ortho*-halogen substitution is unfavourable. Generally, the gain of affinity by the bulky benzyl group is accompanied by a loss of ability to activate the receptor, possibly due to reduced flexibility of the complex and thus stabilization of the inactive state.

Docking

With respect to the aryl moiety, most compounds of the present series of $\text{5-HT}_{2A}\text{R}$ partial agonistic arylethylamines represent three different structural classes: indole, quinazolinodione and 2,5-dimethoxyphenyl derivatives. The benzodifurans are ring-closed analogs of the latter. The results of the FRA indicate that the activity contributions of these aryl fragments differ by only ~ 0.8 log units (ranging from 0.95 for quinazolinodione to 1.75 for 2,5-dimethoxyphenyl). Furthermore, 5-methoxyindole compounds fit well to the QSAR model if the 5-OMe substituent is merged into one variable with that in 2,5-dimethoxyphenyl derivatives, and the effect of a benzyl group as R^N is similar in each structural class. Therefore an overlapping binding mode of the different partial agonists is suggested which can be derived from docking of one representative compound of each class into the $\text{r5-HT}_{2A}\text{R}$ model and which additionally may serve as base for the alignment of all compounds in 3D-QSAR approaches.

Figure 3 shows complexes of the $\text{r5-HT}_{2A}\text{R}$ with the representative compounds **5OH-3**, **21**, and **47**, respectively, after energy optimization. Binding of the arylethylamine moieties depends on three sites, (1) Asp155^{3,32} forming a salt bridge with the protonated amine, (2) a hydrophobic pocket consisting of Phe243^{5,47}, Phe244^{5,48} and Phe340^{6,52}, and (3) serine and threonine residues (Ser159^{3,36}, Thr160^{3,37}, Ser239^{5,43}) as possible hydrogen bond acceptors or donors. In the $\text{h5-HT}_{2A}\text{R}$, a serine replaces Ala242^{5,46}. A hydrogen bond of this serine residue with the indolyl NH moiety is suggested to account for the higher affinity of 5-HT and tryptamine for the $\text{h5-HT}_{2A}\text{R}$ compared to the $\text{r5-HT}_{2A}\text{R}$ [26].

The close and planar alignment of the aryl moieties covering TMs 5 and 6 is enforced by a “phenylalanine pocket”. Binding of many agonists, including 5-HT, 5-methoxytryptamine, DOB, DOI (4-Br- and 4-I-2,5-dimethoxyamphetamine, respectively) and R^N -substituted

dimethoxyphenethylamines is strongly reduced on a Phe340Leu mutant [7, 29, 43, 44]. That Phe243Ala mutation increases and Phe244Ala mutation decreases DOI affinity [28] may be reflected by projection of the 4-Br substituent of compound **21** onto Phe243^{5,47} and Phe244^{5,48} (Fig. 3b). Phe243 represents the bottom of the binding site. The resulting hydrophobic interactions may be conserved in the case of an Phe243Ala mutation. Interestingly, both alanine mutants reduce the affinity of the quinazolinone ketanserin (5-HT_{2A}R antagonist) [28], indicating that the phenyl moiety of cpd. **47** also approaches the phenylalanines 243 and 244. Both residues seem to be important also in the active state of the 5-HT_{2A}R, since the alanine mutations strongly reduce the intrinsic activity of full indole-type agonists [28].

For 5-HT, two alternative hydrogen bonds of Ser239^{5,43} with either the indole NH [28] or the 5-OH group [27] have been suggested. Among the resulting binding modes, the latter is more probable since a Ser239Ala mutant reduces the affinity of 5-HT tenfold whereas the binding of tryptamine, 5-methoxytryptamine, ketanserin and DOI is less affected. An H bond of the 5-OMe groups in 5-methoxytryptamine

and DOI with Ser239 may be replaced by a hydrophobic or dispersion interaction with Ala239 in the mutant. Additionally, different rotamers of N343^{6,55} could act as H bond donors or acceptors for 5-OMe and 5-OH substituents, respectively. The FRA results indicate an alignment of the 5-OMe groups of the indole and dimethoxyphenyl derivatives which is optimal in close proximity to Ser239^{5,43} and N343^{6,55}.

A putative interaction of the indole NH with Ser242^{5,46} was derived from the finding that 5-HT and tryptamine are more affine at the human than at the rat 5-HT_{2A}R (Ala242) [26]. The question is whether Ser159^{3,36} and/or Thr160^{3,37} may stand in for this interaction in the case of the rat receptor. In the complex of the r5-HT_{2A}R with 5OH-3 (Fig. 3a), only Thr160 approaches the indole NH (NH-O distance 2.9 Å). From results on Ser159Ala mutants, a charge-assisted H bond of the hydroxy oxygen with the protonated amino group of 5-HT was suggested [25]. This could indeed be possible in the case of primary amines, but is unlikely with *R*^N substituents and does not correspond to the experimental binding modes of secondary amines to β 1- and β 2-adrenoceptors [15, 16, 45]. In particular, the

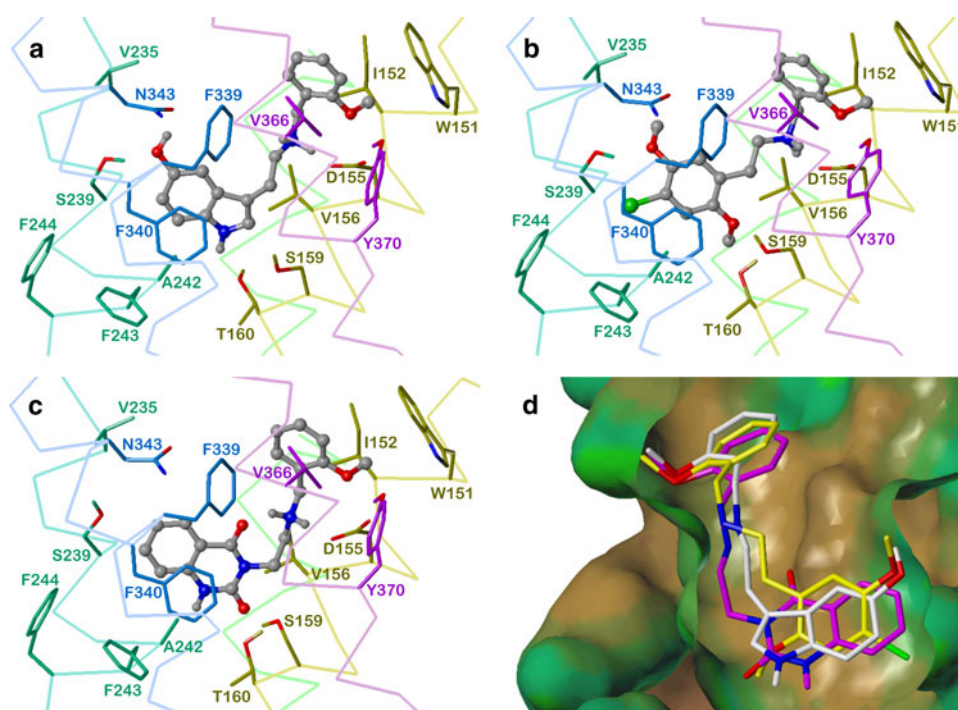


Fig. 3 Docking of ligands representative for subsets **I**, **P** and **Q** into the r5-HT_{2A}R model. **a** compound 5OH-3 (**I**), **b** compound **21** (**P**), **c** compound **47** (**Q**); backbones (C α trace as pale lines), C atoms and some essential hydrogens of the amino acids of TM3-yellow, TM4-green, TM5-greenblue, TM6-blue, TM7-violet; nitrogens—blue, oxygens—red, C and H atoms of the ligands—grey; shown are side chains and labels of residues within 3 Å around the ligands. **d** alignment of the ligand-receptor complexes based on superposition of the backbone atoms of residues within 3 Å around the ligands; C

and essential H atoms of compounds 5OH-3—white, **21**—yellow, **47**—violet; binding site represented by the lipophilic potential (protein variant with the new Crippen parameter table [48, 49]) mapped onto a MOLCAD Connolly surface (J. Brickmann et al. Tech. Univ. Darmstadt, Germany), brown—hydrophobic areas, green and blue—polar areas; for illustration of the hydrophobic pocket being among TMs 3, 5, 6 and 7, the view is vertically rotated by $\sim 180^\circ$ compared to **a-c**

necessary folded conformation of the ethylamine side chain impedes fitting of R^N -benzyl substituents to any suitable receptor site. The models in Fig. 3b and c suggest that Ser159^{3,36} acts as donor in H bonds with the 2-OMe group of dimethoxyphenyl compounds and with a quinazoline-dione oxygen, respectively. The quinazoline NH may form an additional H bond with Thr160^{3,37}.

The docking pose of the R^N benzyl group was derived from the finding that Phe339Leu mutation does not significantly affect the binding of primary amines like 5-HT and DOI, whereas compounds like ketanserin [29] and R^N -substituted 2,5-dimethoxyphenethylamines [7] show strongly reduced affinity. In Fig. 3, the phenyl rings of R^N align perpendicularly with Phe339^{6,51} which forms, together with Trp151^{3,28}, Ile152^{3,29} and Val366^{7,39}, a hydrophobic pocket for the benzyl substituents. The FRA results indicate that an oxygen in ortho position of the phenyl moiety (2-OH, 2-OMe) further enhances activity. This is reflected by an H bond with the OH group of Tyr370^{7,43}.

Figure 3d shows the alignment of the ligands 5OH-3, 21, and 47 within the r5-HT_{2A}R binding site, represented by its lipophilic potential. A nearly continuous hydrophobic “wall” formed by TMs 5, 6 and 7 becomes obvious. Thus, hydrophobic interactions should dominate the QSAR of the present series of 5-HT_{2A}R partial agonistic aryethylamines.

The docking modes of partial agonists shown in Fig. 3 were based on an inactive state model of the r5-HT_{2A}R. This could be a potential source of errors although the recently solved structure of opsin in its G-protein interacting conformation [46] indicated that the topology in the binding site region of the TMs is not essentially different between active and inactive states. Furthermore, the present series consists of mainly weak partial agonists for which interaction with the inactive state should play a significant role. Nevertheless, subtle changes of the binding site during receptor activation may lead to different interactions compared to the inactive state. In particular, an

inward move of TM5 could be possible, leading to closer contacts of the phenylalanines Phe243^{5,47} and Phe244^{5,48} with the aryl moieties.

The docking poses of compounds 5OH-3, 21, and 47 provided the templates for the other ligands of the structural classes **I**, **P** and **Q**, respectively. To obtain an alignment of the whole series, the remaining 48 derivatives were generated by structural modification of the templates. Each ligand replaced its template in the corresponding pre-optimized r5-HT_{2A}R model, and the complexes were refined by subset minimization considering the ligand and a receptor region 6 Å around. Result was a superposition of 51 ligand-r5-HT_{2A}R complexes. For 3D-QSAR approaches, the alignment of the series was achieved by extraction of the ligands. Such alignments “constrained by a binding site” may lead to reasonable interpretations of significant interaction regions [42].

To validate this “direct” mode of structure-based alignment, the pEC₅₀ values were correlated with the Sybyl DOCK energy, roughly representing the binding enthalpy of the ligands. Table 3 indicates that there is indeed a sufficient correlation, in particular, if the steric and electronic terms are individually considered. In this case, 65.3% of the data variance is explained by the docking energy. The intercept is not significant. However, hydrophobic effects that play an important role in particular on binding of the aryl moieties are not directly reflected by the steric and electronic terms. Therefore, log *P* values of the aryl fragments were also included in the correlations. With log *P* in addition to the steric and electronic energy, the correlation was significantly improved. Now, 75.2% of the data variance are explained, all descriptors are significant (*p* < 0.05), and the intercept is close to zero. The residual errors indicate that the models are precise within ~1 log unit. In conclusion, the present structure-based alignment indeed reflects the r5-HT_{2A}R partial agonistic activity of the aryethylamines at a sufficient level of accuracy.

Table 3 Correlation of pEC₅₀ with Sybyl DOCK energies and log *P* (aryl moiety)

	Intercept ^a	Steric ^a	Electronic ^a	DOCK energy ^a	log <i>P</i> ^a	<i>r</i> ²	<i>s</i>	<i>t</i> / <i>F</i> ^b
1	3.45 ± 1.48	−0.151 ± 0.056				0.373	1.318	5.4
2	2.73 ± 2.25		−0.073 ± 0.036			0.259	1.432	4.1
3	−1.10 ± 2.10			−0.096 ± 0.024		0.575	1.086	8.1
4	3.65 ± 0.88				1.38 ± 0.31	0.615	1.033	8.8
5	−1.41 ± 1.92	−0.155 ± 0.042	−0.076 ± 0.025			0.653	0.991	92.0
6	2.34 ± 1.10	−0.078 ± 0.045			1.12 ± 0.32	0.693	0.932	110.6
7	2.65 ± 1.61		−0.022 ± 0.029		1.24 ± 0.36	0.631	1.021	84.1
8	0.34 ± 1.86			−0.053 ± 0.027	0.88 ± 0.38	0.709	0.908	119.3
9	−0.07 ± 1.76	−0.103 ± 0.043	−0.043 ± 0.026		0.77 ± 0.36	0.752	0.847	72.7

^a Regression coefficients ± 95% confidence intervals

^b Results from *t*- and *F*-tests (univariate and multiple regression, respectively)

3D-QSAR

CoMFA [35] and CoMSIA [36] approaches were used to study the QSAR of 5-HT_{2A}R partial agonistic aryethylamines by correlating pEC₅₀ values with field variables. The dependence of pEC₅₀ on the steric and electrostatic docking energy (see Table 3) suggests that CoMFA potentials are appropriate. However, hydrophobic effects identified to be essential on binding (see above) are not considered in CoMFA at the 3D level so that CoMSIA was additionally applied.

Validation and statistics of the models

In a first step, the field types and numbers of principal components (PCs) leading to optimal predictivity of the models were investigated (Table 4). Maximal internal (leave-one-out crossvalidation of the training set) and maximal external predictivity (test set) were individually identified according to the well-known discrepancy between q^2 and r^2_{pred} [41, 47]. In most cases, the test set needs a lower number of PCs than the training set. In terms of q^2 and r^2_{pred} , the predictivity of the best models is rather high (0.8–0.9), but this is in part due to the large data

variance. However, also the errors (s_{PRESS} and s_{pred}) of 0.6–0.85 log units indicate sufficient predictivity.

CoMFA resulted in three nearly equivalent models. There is no significant difference if steric and electrostatic fields are used, if log P of the aryl moieties is additionally considered, or if log P is combined with the steric field. In CoMSIA approaches, the model with all fields (H: hydrophobic, S: steric, E: electrostatic, D: H-donor, A: H-acceptor) was slightly better than all reduced models, but the contributions of S and E to the explained variance were rather low ($\sim 10\%$). Therefore, the hydrophobic field with the highest contribution of $\sim 40\%$ was assumed to be essential, and other fields are added in a combinatorial approach. The best two-field model with respect to internal predictivity resulted from the combination of H and E (contributions $\sim 75\%/25\%$), but in this case the external predictivity was reduced to ~ 0.8 . Addition of the H-donor and the H-acceptor fields, respectively, improved the prediction of the test set similarly. However, the role of the H-donor field is ambiguous. Its influence strongly dominates in the common region of the protonated amino group, indicating that rather the small positional differences in the alignment of the three aryl classes (see Fig. 3) than structural effects are reflected. Another advantage of

Table 4 Dependence of CoMFA and CoMSIA results on the fields and the number of PCs

Fields ^a	PCs	Maximal internal predictivity ^b						PCs	Maximal external predictivity ^c					
		q^2	s_{PRESS}	r^2	s	r^2_{pred}	s_{pred}		q^2	s_{PRESS}	r^2	s	r^2_{pred}	s_{pred}
CoMFA														
SE ^d	7	0.827	0.760	0.979	0.266	0.840	0.672	5	0.795	0.799	0.950	0.395	0.852	0.648
log P SE	7	0.839	0.732	0.976	0.286	0.865	0.617	5	0.793	0.804	0.946	0.410	0.886	0.567
log P S	6	0.828	0.745	0.965	0.338	0.846	0.658	5	0.810	0.770	0.945	0.414	0.866	0.614
log P E	8	0.748	0.935	0.952	0.406	0.748	0.841	3	0.668	0.985	0.829	0.706	0.811	0.729
CoMSIA														
All	8	0.812	0.807	0.968	0.332	0.787	0.774	4	0.733	0.897	0.894	0.565	0.895	0.544
HSED	8	0.810	0.811	0.978	0.279	0.798	0.754	4	0.741	0.884	0.907	0.529	0.867	0.612
HEDA	8	0.802	0.829	0.963	0.356	0.809	0.734	4	0.758	0.854	0.897	0.558	0.890	0.557
HSD	7	0.802	0.813	0.958	0.374	0.769	0.806	4	0.733	0.898	0.900	0.550	0.859	0.631
HED	7	0.798	0.822	0.958	0.375	0.811	0.729	4	0.734	0.895	0.908	0.528	0.871	0.602
HEA ^d	5	0.772	0.843	0.917	0.509	0.876	0.591	5 ^e						
HS	6	0.776	0.849	0.945	0.421	0.717	0.893	4	0.744	0.879	0.914	0.510	0.791	0.767
HE	7	0.790	0.838	0.959	0.370	0.756	0.829	5	0.757	0.871	0.924	0.487	0.805	0.740
HD	7	0.773	0.870	0.947	0.420	0.803	0.744	4	0.722	0.916	0.897	0.557	0.859	0.629
HA	4	0.784	0.806	0.878	0.607	0.827	0.697	5	0.774	0.839	0.892	0.581	0.867	0.612
H	3	0.749	0.856	0.862	0.635	0.780	0.787	3 ^e						

^a S Steric, E electrostatic, H hydrophobic, D H-donor, A H-acceptor

^b Minimum of s_{PRESS} from leave-one-out crossvalidation of the training set

^c Maximum of r^2_{pred} from predictions of the test set

^d Selected for detailed analysis

^e Corresponding to maximal internal predictivity

the HEA model is that both maximal internal and external predictivity result at 5 PCs. The best four-field models were nearly equivalent with the use of all fields. However, compared to the HEA model, the higher degree of complexity (optimal number of 8 PCs) improved internal predictivity by only 0.03 q^2 units.

In conclusion, the CoMFA-SE and CoMSIA-HEA models with 5 PCs were selected for detailed statistical analysis (Table 5) and interpretation of the 3D-QSAR. With the intention to test the consistency of the training series and to estimate the degree of redundancy within the structure–activity relationships, crossvalidation with three groups (leave-12-out) and progressive scrambling [40] were performed. On average, the results from leave-12-out approaches were only slightly inferior to those from leave-one-out crossvalidation. In the CoMFA-SE model, the variability of q^2 and s_{PRESS} and the number of PCs were higher than in the CoMSIA-HEA model. Generally, the predictions of the selected test set were better than any crossvalidation of the training series, indicating a certain

but negligible imbalance of the classification. At a critical r_{yy}^2 (correlation of original and scrambled data) of 0.85, progressive scrambling resulted in derivatives of q^2 (leave-one-out) with respect to r_{yy}^2 close to 1 (<1.2). Thus, the degree of redundancy within both models of the training series is sufficiently low. It should be noted that consideration of the whole series of all 51 compounds does not increase the redundancy if five PCs are used ($dq^2/dr_{yy}^2 = 1.087$ for CoMFA, 1.053 for CoMSIA). However, the derivatives increase up to 2.278 (CoMFA) and 1.527 (CoMSIA), respectively, in the case of the “optimal” number of nine PCs.

The 3D-QSAR will be analyzed by the final models of the training series. CoMFA-SE resulted in a higher r^2 than CoMSIA-HEA (0.95 vs. 0.917). The steric and the hydrophobic fields, respectively, were predominant. In CoMSIA, “electronic” effects seem to be equally distributed over the electrostatic and the acceptor field. Analysis of the differences between experimental and calculated pEC₅₀ values (Table 1) indicated only two outliers ($\Delta > \sim 2$ s): in the CoMFA-SE model compound **17** bearing an α -Me group, and in the case of CoMSIA-HEA compound **9**, the least active primary amine of the series. The predictions of the test set were in particular insufficient (abs $\Delta > 1$) for compounds **25** (CoMFA-SE) and **48** (both models). Since also these structures bear a methyl group as R^2 or R^3 , it seems that the effect of methyl substituents in both positions is not as consistent as assumed by the alignment. This corresponds to the fragment regression analysis with also ambiguous roles of methyl groups.

Discussion of the 3D-QSAR

The stereo views in Fig. 4 show the contour maps from the CoMFA-SE and CoMSIA-HEA models together with an alignment of compounds **8** (**I**), **21** (**P**) and **47** (**Q**) and with the r5-HT_{2A} binding site. With respect to the steric CoMFA field, two spacious green regions are displayed where bulk increases activity. The first region reflects the fit of the aryl moieties to the hydrophobic pocket consisting of the phenylalanines Phe243^{5,47}, Phe244^{5,48} and Phe340^{6,52}. The second one is due to the interaction of the benzyl groups (R^N) mainly with Phe339^{6,51}. A yellow region close to R^4 indicates decreasing activity in the case of an ethoxy substituent (compound **50**). Furthermore, the (*R*)-methyl groups of the distomers **22** and **28** are directed to this contour. Probably the space is restricted by the residues Trp151^{3,28} and Ile152^{3,29}.

The electrostatic region is more fragmented. A red contour close to the *para* position of the phenethylamines describes the activity-enhancing effect of negatively charged halogens and methoxy groups. The suggested hydrogen bonds of 5-methoxy substituents with Ser239^{5,43}

Table 5 Results and validation of the selected 3D-QSAR models

	CoMFA SE 5 PCs	CoMSIA HEA 5 PCs
Leave-one-out crossvalidation		
q^2	0.795	0.772
s_{PRESS}	0.799	0.843
Leave-12-out crossvalidation (3 groups)		
PCs	5–9	3–6
q^2	0.647–0.838	0.718–0.817
mean (q^2)	0.763	0.769
s (q^2)	0.050	0.028
s_{PRESS}	0.764–1.025	0.743–0.938
mean (s_{PRESS})	0.878	0.836
s (s_{PRESS})	0.087	0.051
Progressive scrambling—statistics at critical r_{yy}^2 of 0.85 ^a		
q^2	0.590	0.642
s_{DEP}	1.125	1.044
dq^2/dr_{yy}^2 ^b	1.072	1.009
Final models of the training series		
r^2	0.950	0.917
s	0.395	0.509
F	113.6	66.2
contribution [%] ^c	S 57.5, E 42.5	H 53.6, E 21.9 A 24.5
Predictions of the test set		
r_{pred}^2	0.852	0.876
s_{pred}	0.648	0.591

^a Correlation of original and scrambled pEC₅₀ data

^b Derivative of the fitted function $q^2 = f(r_{yy}^2)$

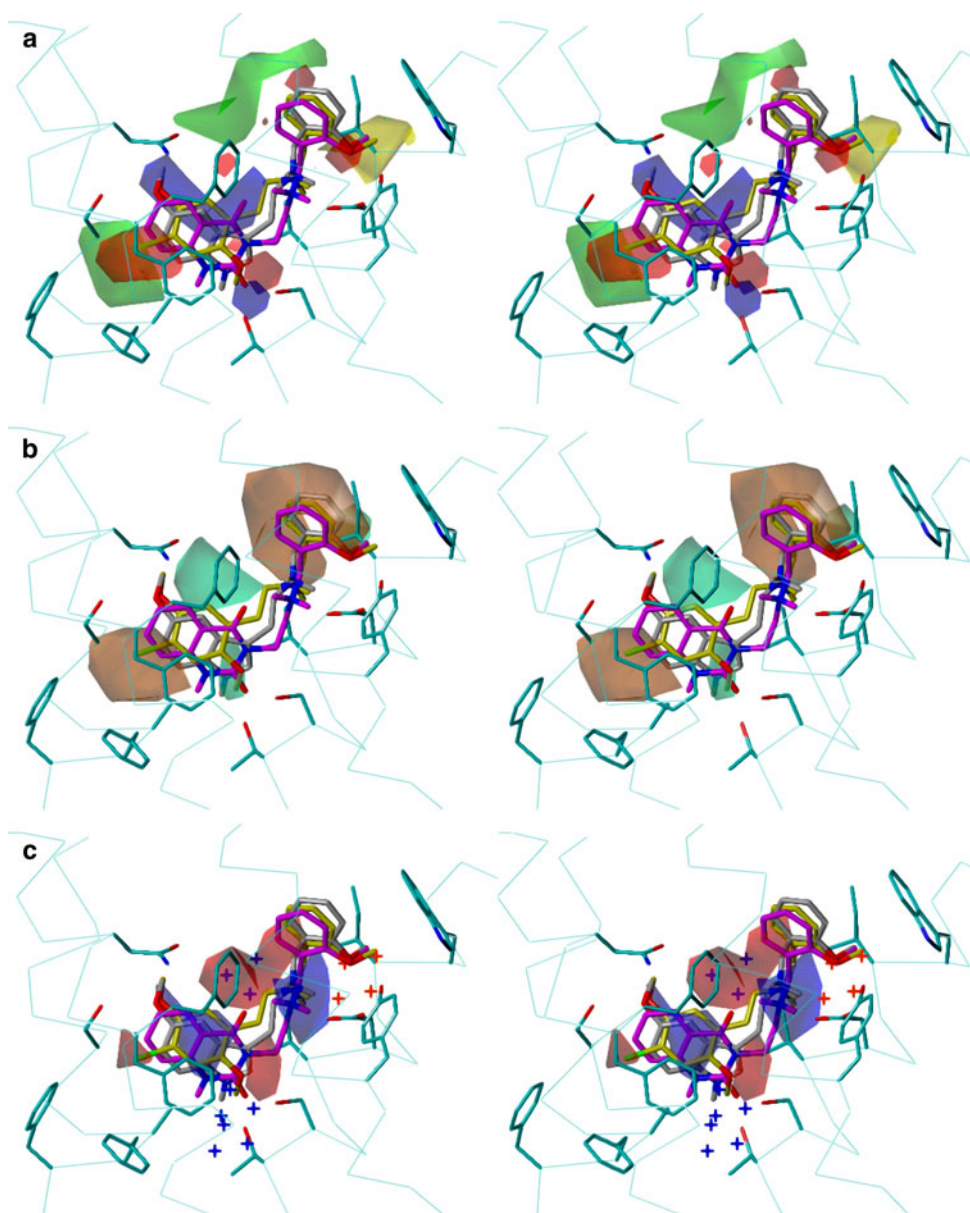
^c S Steric, E electrostatic, H hydrophobic, A H-acceptor

and/or N343^{6,55} are not clearly evident since the red contour is in contrast to the blue one covering the 5-position. This blue region additionally reflects the generally lower activity of quinazolinone derivatives by colocalization with the 4-oxygen. The small red contour above the 6-position of phenethylamines suggests hydrogen bonds of 6-methoxy substituents (compounds **34** and **37**) with N343^{6,55}. The lower red and blue regions are close to the indolyl NH of compound **8** and the 2-methoxy group of compound **21**, respectively. In the latter case, the proposed hydrogen bond with Ser159^{3,36} is reflected. For quinazolinones, the blue contour correlates with the low activity due to overlap with the 2-oxygen. The R^N site contains two red contours. The lower one represents the activity-enhancing effect of 2-hydroxy and 2-methoxy substituents

and corresponds to the suggested hydrogen bond with Tyr370^{7,43}. The upper region is not related to structural variation.

In the CoMSIA-HEA model, two spacious hydrophobic regions predominate (Fig. 4b). Replacing the CoMFA steric field, the left contour depicts the fit of the aryl moieties to the hydrophobic “phenylalanine pocket”. The other contour covers the benzyl group, is surrounded by the side chains of Trp151^{3,28}, Ile152^{3,29}, Val156^{3,33}, Phe339^{6,51} and Val366^{7,39} and represents therefore a second hydrophobic site. Two regions where polar, hydrophilic groups increase activity are placed above and below the aryl moieties, corresponding to the location of the indolyl NH (structural class **I**), 2- and 6-methoxy substituents (**P**) and the quinazolinone oxygens (**Q**). Another

Fig. 4 Stereo views (parallel mode) of the 3D-QSAR contour maps projected into the r5-HT_{2A}R binding site with aligned ligands **8** (**I**), **21** (**P**) and **47** (**Q**); C and some essential H atoms of compounds **8**—grey, **21**—yellow, **47**—violet, backbones (C α trace as lines) and side chain C atoms of binding site residues—cyan, nitrogens—blue, oxygens—red; **a** CoMFA, steric field (green—bulk favourable, yellow—bulk unfavourable, SD*Coeff limits ± 0.05), electrostatic field (blue—positive charge favourable, red—negative charge favourable, SD*Coeff limits ± 0.05); **b** CoMSIA, hydrophobic field (brown—hydrophobic favourable, greenblue—polar favourable, SD*Coeff limits ± 0.03); **c** CoMSIA, electrostatic field (blue—positive charge favourable, red—negative charge favourable, SD*Coeff limits ± 0.015), H-bond acceptor field (represented as crosshairs, orange—acceptor favourable, blue—acceptor unfavourable, SD*Coeff limits ± 0.03)



polar contour close to the *ortho* position of the benzyl groups is probably due to the negative effect of a 2-Br or 2-ethoxy substituent (compounds **44** and **50**).

The electrostatic contours must be analyzed together with the influence of the H-acceptor fields since both effects seem to counteract each other in some regions (Fig. 4c). Like in CoMFA, the red contour near the *para* position of phenethylamines represents the activity-enhancing effect of negatively charged halogens and methoxy groups. Again, a blue region covers the 5-position which does not correspond to hydrogen bonds of 5-methoxy substituents with Ser239^{5,43} and/or N343^{6,55}. However, this region is smaller than in CoMFA. CoMSIA resulted in two larger red contours above and below the aligned structures being colocalized with 2- and 6-methoxy groups of phenethylamines and with the oxygens of quinazolinodione derivatives. But these effects are counterbalanced by the H-acceptor fields, indicating that just in those regions an acceptor atom is unfavourable. Thus, the local QSAR does not directly reflect binding, but rather fit the lower activity of quinazolinodiones to the model. The blue region close to the protonated nitrogens may be attributed to alignment differences between the three structural classes. The mechanistic significance of this effect with respect to the salt bridge with Asp155^{3,32} is questionable. Acceptor atoms are favourable in *ortho* position of benzyl R^N groups, indicating that a hydrogen bond with Tyr370^{7,43} may be formed.

In summary, the results from 3D-QSAR approaches are widely consistent with the docking modes (cf. Figs. 3, 4). In particular, hydrophobic interactions and regions provided by CoMSIA do well correlate with the lipophilic potential of the binding site and with the suggested hydrophobic pockets. The steric field from CoMFA appears to replace the hydrophobic CoMSIA field in the aryl and the R^N region. Therefore, additional consideration of log *P* of the aryl moieties did not improve the correlation (see Table 4). The influence of electrostatic and H-acceptor fields cannot be thoroughly explained by the suggested hydrogen bonds with Ser159^{3,36}, Ser239^{5,43} and N343^{6,55}. In a rather descriptive manner, both fields also discriminate the less active quinazolinodiones from the other structural classes, raising the question whether the docking mode of the quinazolinodione derivatives overestimates putative electrostatic interactions. Possibly, active state models can identify mechanistic reasons for activity differences between the three structural classes in more detail.

Conclusions

A series of 51 5-HT_{2A} partial agonistic arylethylamines (primary or benzylamines) from different structural classes

(indoles, methoxybenzenes, quinazolinodiones) was investigated by different computer methods following a hierarchic program. The data, pEC₅₀ values and intrinsic activities (E_{\max}) on rat arteries, show high variability of pEC₅₀ from 4 to 10 and of E_{\max} from 15 to 70%.

Fragment regression is well suited as preliminary tool to detect which substructures affect potency or intrinsic activity. Analysis of the fragment contributions and properties has led to hypotheses on essential ligand-receptor interactions like binding to hydrophobic pockets and possible hydrogen bonds. Together with data on all available mutants, these hypotheses are appropriate to derive a common binding site for arylethylamines at the r5-HT_{2A}R by receptor modeling.

Docking studies of representative members of each structural class have suggested interaction patterns—hydrogen bonds of the ligands with Ser159^{3,36}, Ser239^{5,43} and N343^{6,55} as well as fit into two hydrophobic pockets consisting of Phe243^{5,47}, Phe244^{5,48} and Phe340^{6,52} on the one and Phe339^{6,51}, Trp151^{3,28}, Ile152^{3,29} and Val366^{7,39} on the other hand.

Docking of the other ligands using the three representative structures as templates and minimization of the complexes has provided an alignment for 3D-QSAR approaches based on the superposition of the ligands in their putative bioactive conformation within the binding site. An additional validation of this procedure is that the pEC₅₀ values correlate well with the Sybyl docking energy and the hydrophobicity of the aryl moieties.

With this alignment, 3D-QSAR methods (CoMFA and CoMSIA) using a training set of 36 and a test set of 15 compounds have led to a more detailed exploration of the structure–activity relationships. The pEC₅₀ values correlate with steric, electrostatic, hydrophobic and H-bond acceptor fields, indicated by sufficient fit (r^2 : 0.92–0.95), internal (q^2 : 0.75–0.8) and external predictivity (r^2_{pred} : 0.85–0.88). The final models with five PCs do not suffer from structural redundancy as indicated by progressive scrambling. The important interaction regions largely reflect the patterns provided by the putative binding site. In particular, the fit of the aryl moiety and the benzyl substituent, respectively, to the two hydrophobic pockets is evident. Also the putative hydrogen bonds of the indole and methoxybenzene derivatives are partially reflected. In the case of the quinazolinodiones, the role of specific electrostatic interactions is rather ambiguous.

In summary, the application of fragment regression, receptor modeling, docking and 3D-QSAR approaches has led to conclusive hypotheses on ligand-r5-HT_{2A}R interactions and to models explaining the partial agonistic potency of phenethylamines and enabling the prediction of novel 5-HT_{2A}R agonists.

Acknowledgments This work was supported by the Graduate Training Program (Graduiertenkolleg) GRK 760, “Medicinal Chemistry: Molecular Recognition - Ligand-Receptor Interactions”, of the Deutsche Forschungsgemeinschaft.

References

- Peroutka SJ (1990) 5-Hydroxytryptamine receptor subtypes. *Pharmacol Toxicol* 67:373–383
- Rapport MM, Green AA, Page IH (1947) Purification of the substance which is responsible for vasoconstrictor activity of serum. *Fed Proc* 6:184
- Rapport MM, Green AA, Page IH (1948) Serum vasoconstrictor (serotonin): isolation and characterization. *J Biol Chem* 176:1243–1251
- Roth BL, Willins DL, Kristiansen K, Kroeze WK (1998) 5-Hydroxytryptamine₂-family receptors (5-hydroxytryptamine_{2A}, 5-hydroxytryptamine_{2B}, 5-hydroxytryptamine_{2C}): where structure meets function. *Pharmacol Ther* 79:231–257
- Zifa E, Fillion G (1992) 5-Hydroxytryptamine Receptors. *Pharmacol Rev* 44:401–457
- Nichols DE, Nichols CD (2008) Serotonin receptors. *Chem Rev* 108:1614–1641
- Braden MR, Parrish JC, Naylor JC, Nichols DE (2006) Molecular interaction of serotonin 5-HT_{2A} receptor residues Phe339(6.51) and Phe340(6.52) with superpotent N-benzyl phenethylamine agonists. *Mol Pharmacol* 70:1956–1964
- Heim R (2003) Synthesis and pharmacology of potent 5-HT_{2A} receptor agonists with N-2-methoxybenzyl partial structure. Dr. rer. nat. PhD Thesis, Free University, Berlin
- Elz S, Kläß T, Warnke U, Pertz HH (2002) Development of highly potent partial agonists and chiral antagonists as tool for the study of 5-HT_{2A}-receptor mediated function. *Naunyn-Schmiedeberg's Arch Pharmacol* 365:R29
- Halter CC (2004) Mescaline analogs as partial 5-HT_{2A} receptor agonists: Synthesis and pharmacological in vitro testing. Dipl. chem. Diploma thesis, University Regensburg, Regensburg
- Heim R, Pertz HH, Walther I, Elz S (1998) Congeners of 3-(2-Benzylaminoethyl)-2, 4-quinazolidione: partial agonists for rat vascular 5-HT_{2A} receptors. *Naunyn-Schmiedeberg's Arch Pharmacol* 358:R105
- Heim R, Pertz HH, Zabel M, Elz S (2002) Stereoselective synthesis, absolute configuration and 5-HT_{2A} agonism of chiral 2-methoxybenzylamines. *Arch Pharm Pharm Med Chem* 335:82
- Pertz HH, Heim R, Elz S (2000) N-benzylated phenylethanamines are highly potent partial agonists at 5-HT_{2A} receptors. *Arch Pharm Pharm Med Chem* 333:30
- Ratzeburg K, Heim R, Mahboobi S, Henatsch J, Pertz HH, Elz S (2003) Potent partial 5-HT_{2A}-receptor agonism of phenylethanamines related to mescaline in the rat tail artery model. *Naunyn-Schmiedeberg's Arch Pharmacol* 367:R31
- Cherezov V, Rosenbaum DM, Hanson MA, Rasmussen SG, Thian FS, Kobilka TS, Choi HJ, Kuhn P, Weis WI, Kobilka BK, Stevens RC (2007) High-resolution crystal structure of an engineered human beta₂-adrenergic G protein-coupled receptor. *Science* 318:1258–1265
- Rasmussen SG, Choi HJ, Rosenbaum DM, Kobilka TS, Thian FS, Edwards PC, Burghammer M, Ratnala VR, Sanishvili R, Fischetti RF, Schertler GF, Weis WI, Kobilka BK (2007) Crystal structure of the human beta₂ adrenergic G-protein-coupled receptor. *Nature* 450:383–387
- Gasteiger E, Gattiker A, Hoogland C, Ivanyi I, Appel RD, Bairoch A (2003) ExPASy: the proteomics server for in-depth protein knowledge and analysis. *Nucleic Acids Res* 31:3784–3788
- Wang J, Wolf RM, Caldwell JW, Kollman PA, Case DA (2004) Development and testing of a general amber force field. *J Comput Chem* 25:1157–1174
- Lovell SC, Word JM, Richardson JS, Richardson DC (2000) The penultimate rotamer library. *Proteins* 40:389–408
- Strasser A, Striegl B, Wittmann HJ, Seifert R (2008) Pharmacological profile of histaprodifens at four recombinant histamine H-1 receptor species isoforms. *J Pharmacol Exp Ther* 324:60–71
- Van der Spoel D, Lindahl E, Hess B, Groenhof G, Mark AE, Berendsen HJC (2005) GROMACS: fast, flexible, and free. *J Comput Chem* 26:1701–1718
- Oostenbrink C, Villa A, Mark AE, Van Gunsteren WF (2004) A biomolecular force field based on the free enthalpy of hydration and solvation: the GROMOS force-field parameter sets 53A5 and 53A6. *J Comput Chem* 25:1656–1676
- Sealfon SC, Chi L, Ebersole BJ, Rodic V, Zhang D, Ballesteros J, Weinstein H (1995) Related contribution of specific helix 2 and 7 residues to conformational activation of the serotonin 5-HT_{2A} receptor. *J Biol Chem* 28:16683–16688
- Wang CD, Gallaher TK, Shih JC (1993) Site-directed mutagenesis of the serotonin 5-hydroxytryptamine₂ receptor: identification of amino acids necessary for ligand binding and receptor activation. *Mol Pharmacol* 43:931–940
- Almaula N, Ebersole BJ, Zhang D, Weinstein H, Sealfon SC (1996) Mapping the binding site pocket of the serotonin 5-Hydroxytryptamine_{2A} receptor. Ser3.36(159) provides a second interaction site for the protonated amine of serotonin but not of lysergic acid diethylamide or bufotenin. *J Biol Chem* 271:14672–14675
- Johnson MP, Loncharich RJ, Baez M, Nelson DL (1994) Species variations in transmembrane region V of the 5-hydroxytryptamine type 2A receptor alter the structure-activity relationship of certain ergolines and tryptamines. *Mol Pharmacol* 45:277–286
- Johnson MP, Wainscott DB, Lucaites VL, Baez M, Nelson DL (1997) Mutations of transmembrane IV and V serines indicate that all tryptamines do not bind to the rat 5-HT_{2A} receptor in the same manner. *Molecular Brain Research* 49:1–6
- Shapiro DA, Kristiansen K, Kroeze WK, Roth BL (2000) Differential modes of agonist binding to 5-hydroxytryptamine(2A) serotonin receptors revealed by mutation and molecular modeling of conserved residues in transmembrane region 5. *Mol Pharmacol* 58:877–886
- Choudhary MS, Craigo S, Roth BL (1993) A single point mutation (Phe340→Leu340) of a conserved phenylalanine abolishes 4-[125I]iodo-(2, 5-dimethoxy)phenylisopropylamine and [3H]mesulergine but not [3H]ketanserin binding to 5-hydroxytryptamine₂ receptors. *Mol Pharmacol* 43:755–761
- Choudhary MS, Sachs N, Uluer A, Glennon RA, Westkaemper RB, Roth BL (1995) Differential ergoline and ergopeptine binding to 5-hydroxytryptamine_{2A} receptors: ergolines require an aromatic residue at position 340 for high affinity binding. *Mol Pharmacol* 47:450–457
- Ballesteros JA, Weinstein H (1995) Integrated methods for the construction of three-dimensional models and computational probing of structure-function relations in G protein-coupled receptors. *Methods Neurosci* 25:366–428
- Clark M, Cramer I RD, Van Opdenbosch N (1989) Validation of the general purpose tripos 5.2 force field. *J Comp Chem* 10:982–1012
- Glennon RA, Westkaemper RB, Bartyzel P (1991) Serotonin receptor subtypes: basic and clinical aspects. In: Venter CJ, Harrison LC, Peroutka SJ (eds) *Receptor biochemistry and methodology*. Wiley-Liss, New York, pp 19–64
- Giger R (1989) *Actual Chim Ther* 16:151–186

35. Cramer I RD, Patterson DE, Bue JD (1988) Comparative molecular field analysis (CoMFA): effect of shape on binding of steroids to carrier protein. *J Am Chem Soc* 110:5959–5967
36. Klebe G, Abraham U, Mietzner T (1994) Molecular similarity indices in a comparative analysis (CoMSIA) of drug molecules to correlate and predict their biological activity. *J Med Chem* 37:4130–4146
37. Folkers G, Merz A, Rognan D (1993) CoMFA: Scope and Limitations. In: Kubinyi H (ed) 3D QSAR in drug design: theory, methods and applications. ESCOM, Leiden, pp 583–618
38. Wold S, Ruhe A, Wold H, Dunn WJ (1984) The covariance problem in linear regression. The partial least squares (PLS) approach to generalized inverses. *SIAM J Sci Stat Comp* 5:735–743
39. Cramer I RD, Bue JD, Petterson DE (1988) Crossvalidation, bootstrapping, and partial least squares compared with multiple regression in conventional QSAR studies. *Quant Struct-Act Relat* 7:18–25
40. Clark RD, Fox PC (2004) Statistical variation in progressive scrambling. *J Comput Aided Mol Des* 18:563–576
41. Golbraikh A, Tropsha A (2002) Beware of $q(2)!$. *J Mol Graph Model* 20:269–276
42. Doweiko AM (2004) 3D-QSAR illusions. *J Comput Aided Mol Des* 18:587–596
43. Roth BL, Choudhary MS, Khan N, Uluer AZ (1997) High-affinity agonist binding is not sufficient for agonist efficacy at 5-hydroxytryptamine_{2A} receptors: evidence in favor of a modified ternary complex model. *J Pharmacol Exp Ther* 280:576–583
44. Roth BL, Shoham M, Choudhary MS, Khan N (1997) Identification of conserved aromatic residues essential for agonist binding and second messenger production at 5-hydroxytryptamine_{2A} receptors. *Mol Pharmacol* 52:259–266
45. Warne T, Serrano-Vega MJ, Baker JG, Moukhametzianov R, Edwards PC, Henderson R, Leslie AGW, Tate CG, Schertler GFX (2008) Structure of a β_1 -adrenergic G-protein-coupled receptor. *Nature* 454:U482–U486
46. Scheerer P, Park JH, Hildebrand PW, Kim YJ, Krauss N, Choe HW, Hofmann KP, Ernst OP (2008) Crystal structure of opsin in its G-protein-interacting conformation. *Nature* 455:497–503
47. Kubinyi H, Hamprecht FA, Mietzner T (1998) Three-dimensional quantitative similarity-activity relationships (3D QSiAR) from SEAL similarity matrices. *J Med Chem* 41:2553–2564
48. Ghose AK, Viswanadhan VN, Wendoloski JJ (1998) Prediction of Hydrophobic (Lipophilic) Properties of Small Organic Molecules Using Fragmental Methods: An Analysis of ALOGP and CLOGP Methods. *J Phys Chem* 102:3762–3772
49. Heiden W, Moeckel G, Brickmann J (1993) A new approach to analysis and display of local lipophilicity/hydrophilicity mapped on molecular surfaces. *J Comput Aided Mol Des* 7:503–514